

Studies of Some New Biologically Active Ligands and Their Complexes Derived from Some Transition Metal Ions

ADEL S. ORABI*, H.K. IBRAHIM, EL-SAYED H. EL-TAMANY and A. RADWAN

Department of Chemistry, Faculty of Science, Suez Canal University, Ismailia, Egypt

E- mail: orabiadel@hotmail.com, orabiadel2005@yahoo.com

The metal complexes derived from new biologically active quinoline derivatives namely; 4-amino-5-(quinolin-8-yloxymethyl)-2,4-dihydro-[1,2,4]triazol-3-thione (**L1**), benzoic acid *N'*-[2-(quinolin-8-yloxy)-acetyl]-hydrazide (**L2**), [4-phenyl-5-(quinolin-8-yloxymethyl)-4H[1,2,4]triazol-3-ylsulfanyl]-acetic acid ethyl ester (**L3**) and [2-(quinolin-8-yloxy)-acetyl]-thiourea (**L4**) were prepared by reacting the quinoline derivatives with nitrates of zinc(II), copper(II), nickel(II), cobalt(II) and iron(III) in ethanolic medium. The metal:ligand ratio was found to be 1:2 by using the standard method of complexometric titration. The Fe(III) % in its complexes was estimated using spectrophotometric method. The structure of the isolated complexes were studied on the basis of their infrared spectra, elemental analysis (C, H, N, H₂O, M %), molar conductivity, thermal analysis (DTA/TG), mössbauer, magnetic susceptibility and computer modeling of the ligands. The mössbauer spectra of the iron complexes reflect the Fe(III) high spin complexes with octahedral structure. The complexes gave higher activity towards the microorganisms under consideration at 50 and 100 ppm rather than the organic ligands.

Key Words: Quinoline derivatives, Mössbauer spectra, Solid complexes, Molecular modeling, Antimicrobial activity.

INTRODUCTION

Quinoline derivatives are well-known as biologically active agents¹⁻⁷, such as antimalaria³, antiseptic amobicial^{4,5}, anthlimintic antihypertensive agents^{6,7}, some others which possess antimicrobial activities⁸, also quinoline derivatives have several uses in many field *i.e.* pharmaceutical and industrial applications⁹⁻¹². Absorption of metal iron in cell membrane increased as metal administered as chelated with 8-hydroxyquinoline¹³, the chelation of Fe with some quinoline derivatives increase its cytotoxicity to humun carcinoma cell, inhibited DNA synthesis of tumor cell at micromolar concentration¹⁴. In industrial field, some complexes of 8-hydroxy

quinoline and its derivatives can be used as the emitting elements in (EL) devices. Where the highly ordered arrangement of emitting molecular may be increase the luminous efficiency of (EL) devices^{15,16}. Quinoline produced mutation in the *Salmonella typhimurium* mutagenicity test in the presence but not in the absence of metabolic activation, produced unscheduled DNA synthesis (UDS) in cultured rat hepatocytes and also produced adducts with RNA and DNA when incubated in the presence of metabolic activation. The quinoline which bonded to nucleic acid was released during incubation at 100 °C under alkaline or acidic conditions as 3-hydroxy quinoline^{17,18}. Collectively, due to the importance of quinoline derivatives and its complexes, we decided to prepare four new quinoline derivatives and their complexes with some transition metal ions which play some role in living cell.

EXPERIMENTAL

All chemicals used in the present study were reagent grade. The solvent used without extra purification. The melting points were measured on a MEL-TEMP II apparatus and corrected using standard benzoic acid. Elemental analysis were carried out using a Heraeus CHN Rapid Analyzer. The conductance measurements of 0.001 M solutions of the complexes in DMSO were performed using a WTW model LF-42 conductivity bridge fitted with a LTA-100 conductivity cell. Thermal analysis of the complexes was carried out on a Perkin-Elmer DTA-7 differential thermal analyzed with a TAC 7/DX controller instrument using a platinum cell under nitrogen atmosphere at a heating rate of 10 °C/min. IR spectra were reported with a Perkin Elmer 1430 with CDS data station using KBr pellets. ¹H NMR and ¹³C NMR measurements were carried out on a Varian Gemini-200 using tetramethyl silane (TMS) as an internal standard. Mass spectra were measured using MSQP 1000EX Shimadzu instrument. Mössbauer spectra of the iron complexes were carried out using Elseint EMS-21 instrument. The water content of the complexes under investigation were carried out using ISOTEMP-300 oven. The magnetic susceptibility of the formed complexes was recorded using Bruker Magnet B-E15 instrument.

Synthesis of 4-amino-5-(quinoline-8-yloxymethyl)-2,4-dihydro-[1,2,4]triazole-3-thione (L1): (Quinolin-8-yloxy)-acetic acid hydrazide (0.01 mol) was refluxed with (0.015 mol) carbon disulphide in absolute ethanol containing (0.01 mol) KOH on the water bath for 1 h. The residual formed was dissolved in water (5 mL) and then treated with hydrazine hydrate (0.02 mol) and refluxed for 4 h. The contents were cooled, diluted with water, acidified with HCl. The precipitate formed was filtered, washed with water, recrystallized from DMF/H₂O mixture and finally dried under vacuum. L1 was found to be as a gray powder (41 % yield) with melting

point 240 °C. Elemental analysis for C₁₂H₁₁N₅OS (m.w., 273) Calcd. %: C, 52.73; H, 4.06; N, 25.62, found %: C, 53.03; H, 3.86; N, 25.41. The ¹H NMR studies gave signals at δ = 14 (s, 1H, NH), 8.8-7.3 (m, 6H, Ar-H), 5.7 (s, 2H, NH₂) and at 5.1 ppm (s, 2H, OCH₂). ¹³C NMR carried out in CDCl₃ solvent gave signal at 166, 60 ppm attributed to C=S, O-CH₂, respectively. The mass spectrum showed the molecular ion peak at m/z = 273 represents the molecular weight.

Synthesis of benzoic acid N'-[2-(quinoline-8-yloxy)acetyl]hydrazide (L2): A mixture of (quinolin-8-yloxy)acetic acid hydrazide (0.01 mol) and benzoyl chloride (0.01 mol) in benzene (30 mL) was refluxed for 4 h. The solid product, which formed after cooling, was washed with sodium bicarbonate solution (10 %) and then with water and recrystallized from ethanol. The white crystal product (61 % yield) was dried under vacuum. The formed L2 ligand has melting point 220 °C and the calculated analytical data as following: The calculated analytical data for C₁₈H₁₅N₃O₃ (m.w. 321), C, 67.28; H, 4.70; N, 13.08: found %: C, 66.96; H, 4.35; N, 12.74. The ¹H NMR studies gave signals at δ = 10.7 ppm (s, 2H, NHNH), 9-7.4 ppm (m, 11H, Ar-H) and 5.0 ppm (s, 2H, CH₂). The ¹³C NMR gave signal at 167, 165 ppm attributed to two C=O groups. The mass spectrum showed the molecular ion peak at m/z = 321 represents the molecular weight.

Synthesis of [4-phenyl-5-(quinoline-8-yloxymethyl)-4H-[1,2,4]-triazole-3-yl-sulfanyl]-acetic acid ethyl ester (L3): A mixture of 4-phenyl-5-(quinolin-8-yloxymethyl)-2,4-dihydro[1,2,4]triazole-3-thion (0.01 mol), anhydrous K₂CO₃ (0.01 mol) and ethyl chloroacetate (0.01 mol) in dry acetone (20 mL) was refluxed for 6 h. On cooling the solid product formed was filtrated, washed and recrystallized from ethanol. The greenish crystal formed (87 % yield) has the following analytical data: C₂₂H₂₀N₄O₃S (m.w. 420), calculated element %, C, 62.78; H, 4.75; N, 13.31; Found: C, 62.60; H, 5.0; N, 13.10. The ¹H NMR studies gave signals at 8.8-7.1 (m, 11H, Ar-H), 5.2 (s, 2H, OCH₂), 4.1 ppm (s, 2H, SCH₂), 4.2-4.1 (q, 2H, CH₂) and 1.2-1.1 ppm (t, 3H, CH₃). The mass spectrum showed the molecular ion peak at m/z = 421.

Synthesis of [2-(quinoline-8-yloxy)-acetyl]-thiourea (L4): 8-Quinoloxoxy acetic acid ethyl ester (0.01 mol) was refluxed with thiourea in ethanol (25 mL) for 6 h. The solid formed product was filtered, washed and recrystallized from ethanol. The pale yellow crystal (70 % yield) C₁₂H₁₁N₃O₂S (m.w. 261) has the following analytical data: calculated, C, 55.16; H, 4.24; N, 16.08: found, C, 54.8; H, 4.0; N, 15.8. The ¹³C NMR gave signal at 183, 168 ppm attributed to C=S, C=O group, respectively. The mass spectrum showed the molecular ion peak at m/z = 261 represents the molecular weight.

Synthesis of the complexes: To the ethanolic solution of the respective ligand (0.002 mol) 0.546 g of L1, 0.642 g of L2, 0.84 g of L3 and 0.522 g of L4 (20 mL), a solution of metal nitrates (0.001 mol) 0.297 g for Zn, 0.241 g for Cu, 0.29 g for Ni, 0.291 g for Co and 0.404 g for Fe nitrates in ethanol (10 mL), was added. The reaction mixture was refluxed under stirring for 1 h. The precipitated complexes were separated by filtration, washed with ethanol and dried in vacuum at room temperature.

RESULTS AND DISCUSSION

The elemental analysis (C, H, N, M) % of the solid complexes show 1:2 (metal:ligand) stoichiometry. These complexes are freely soluble in common polar solvent (ethanol, methanol, H₂O, DMSO, DMF). The complexes are found to be non-hygroscopic powder structure (Tables 1 and 2).

Molar conductance: The molar conductance of the complexes in DMSO (0.001M) (Tables 1 and 2) indicate that all the compounds behave as electrolytes with the structure $A^{2+}.2B^{-}$ for Zn(II), Cu(II), Ni(II) and Co(II) complexes and as $A^{3+}.3B^{-}$ for Fe(III) complexes^{26,33}, where A^{n+} refers to the coordinate- sphere of the formed complexes and B^{-} refer to the ionization sphere ($B = NO_3^{-}$) (**Scheme-II** as an example).

Infrared spectra: The significant IR data of the ligands as well as their metal complexes are listed in Tables 3 and 4. The band at 3670-3200 cm^{-1} which is present in all complexes with one exception for Cu(II)-L1 complex as a medium broad band may be due to coordinated water molecules (**Scheme-II**, as an example).

Ligands bands at 3438, 3260 and 3133 cm^{-1} for L1, 3393, 3225 cm^{-1} for L2, 3391, 3282 and 3146 cm^{-1} for L4 were assigned collectively as $\nu(OH, NH, NH_2)$ ¹⁹. The band appeared at 3394 cm^{-1} for L3 may be due to the enolic form of the carbonyl group which found due to the keto-enol tautomerism. These bands exerted shifts of *ca.* 20-80 cm^{-1} to lower frequencies for complexes of L1, L2 and L4 ligands and disappeared for complexes derived from L3 ligand.

The band at *ca.* 1383 cm^{-1} for all complexes may be due to the stretching vibration of NO_3^{-} group²⁰ in the ionization sphere of the formed complexes, the stretching vibration of the C=S bond appeared at 1114 cm^{-1} for L1 ligand which gave slightly negative shift for the formed complexes indicating the participation of S atom as chelation center, meanwhile this band appeared at 1119 cm^{-1} as strong band for L4 ligand and gave slightly positive shift which denote unsharing of the S atom as complexation site (**Scheme-II**)^{21,22}. The carbonyl group has stretching vibration appeared at 1695 and 1649 cm^{-1} for L2 ligand, 1734 cm^{-1} for L3 ligand and 1748 cm^{-1} for L4 ligand. Generally these bands gave negative shift for the complexes which formed from these ligands with the metal ions under investigation

TABLE-1
 PHYSICAL DATA AND CHEMICAL ANALYSIS OF L1 AND L2 LIGANDS AND THEIR METAL COMPLEXES

Compd.	m.f.	m.w.	Colour	m.p. (°C)	Elemental analysis: Calcd. (Found) %					Conductivity ($\mu\text{moh/cm}$)
					C	H	N	M	H ₂ O	
L1	C ₁₂ H ₁₁ N ₅ OS	273.32	Grey	240	52.73 (53.03)	4.06 (3.86)	25.62 (25.41)	–	–	–
Zn(II)	[Zn(C ₁₂ H ₁₁ N ₅ OS) ₂ (H ₂ O) ₂](NO ₃) ₂	772.07	Brown	>300	37.34 (37.41)	3.39 (3.28)	21.77 (21.57)	8.47 (8.53)	4.62 (4.81)	140
Cu(II)	[Cu(C ₁₂ H ₁₁ N ₅ OS) ₂](NO ₃) ₂	734.19	Green	>300	39.26 (39.10)	3.02 (2.97)	22.89 (22.74)	8.66 (8.42)	–	181
Ni(II)	[Ni(C ₁₂ H ₁₁ N ₅ OS) ₂ (H ₂ O) ₂](NO ₃) ₂	765.37	Green	>300	37.66 (37.44)	3.42 (3.54)	21.96 (21.76)	7.67 (7.34)	4.71 (4.83)	175
Co(II)	[Co(C ₁₂ H ₁₁ N ₅ OS) ₂ (H ₂ O) ₂](NO ₃) ₂	765.61	Light brown	>300	37.65 (37.32)	3.42 (3.37)	21.95 (21.74)	7.70 (7.59)	4.71 (4.79)	188
Fe(III)	[Fe(C ₁₂ H ₁₁ N ₅ OS) ₂ (H ₂ O) ₂](NO ₃) ₃	824.52	Dark green	>300	34.96 (34.71)	3.18 (3.12)	22.08 (22.01)	6.77 (6.81)	4.37 (4.30)	273
L2	C ₁₈ H ₁₅ N ₃ O ₃	321.34	White	220	67.28 (66.96)	4.70 (4.35)	13.08 (12.74)	–	–	–
Zn(II)	[Zn(C ₁₈ H ₁₅ N ₃ O ₃) ₂ (H ₂ O) ₂](NO ₃) ₂	868.10	Yellow	160	49.81 (49.60)	3.95 (3.91)	12.91 (12.71)	7.53 (7.32)	4.15 (4.21)	140
Cu(II)	[Cu(C ₁₈ H ₁₅ N ₃ O ₃) ₂ (H ₂ O) ₂](NO ₃) ₂	866.25	Green	150	49.92 (49.78)	3.96 (3.85)	12.94 (12.79)	7.34 (7.22)	4.16 (4.30)	135
Ni(II)	[Ni(C ₁₈ H ₁₅ N ₃ O ₃) ₂ (H ₂ O) ₂](NO ₃) ₂	861.64	Light green	165	50.20 (50.13)	3.98 (3.71)	13.01 (12.95)	6.81 (6.61)	4.18 (4.31)	115
Co(II)	[Co(C ₁₈ H ₁₅ N ₃ O ₃) ₂ (H ₂ O) ₂](NO ₃) ₂	861.61	Pink	130	50.18 (50.12)	3.98 (3.82)	13.00 (13.01)	6.84 (6.49)	4.18 (4.21)	150
Fe(III)	[Fe(C ₁₈ H ₁₅ N ₃ O ₃) ₂ (H ₂ O) ₂](NO ₃) ₃	920.56	Dark brown	95	46.97 (46.92)	3.72 (3.53)	13.69 (13.61)	6.07 (6.47)	3.91 (3.72)	225

TABLE-2
PHYSICAL DATA AND CHEMICAL ANALYSIS OF L3 AND L4 LIGANDS AND THEIR METAL COMPLEXES

Compd.	m.f.	m.w.	Colour	m.p. (°C)	Elemental analysis: Calcd. (Found) %					Conductivity ($\mu\text{moh/cm}$)
					C	H	N	M	H ₂ O	
L3	$\text{C}_{22}\text{H}_{30}\text{N}_4\text{O}_3\text{S}$	420.49	Pale green	135	62.78 (62.60)	4.75 (5.00)	13.31 (13.10)	–	–	–
Zn(II)	$[\text{Zn}(\text{C}_{22}\text{H}_{30}\text{N}_4\text{O}_3\text{S})_2(\text{H}_2\text{O})_2](\text{NO}_3)_2$	1066.41	Yellow	95	49.56 (49.36)	4.16 (4.06)	13.13 (13.07)	6.13 (6.21)	3.38 (3.34)	200
Cu(II)	$[\text{Cu}(\text{C}_{22}\text{H}_{30}\text{N}_4\text{O}_3\text{S})_2(\text{H}_2\text{O})_2](\text{NO}_3)_2$	1064.57	Green	90	49.64 (49.51)	4.17 (4.32)	13.16 (13.24)	5.97 (6.12)	3.38 (3.51)	100
Ni(II)	$[\text{Ni}(\text{C}_{22}\text{H}_{30}\text{N}_4\text{O}_3\text{S})_2(\text{H}_2\text{O})_2](\text{NO}_3)_2$	1059.71	Green	115	49.87 (49.61)	4.18 (4.21)	13.22 (13.02)	5.54 (5.31)	3.40 (3.43)	135
Co(II)	$[\text{Co}(\text{C}_{22}\text{H}_{30}\text{N}_4\text{O}_3\text{S})_2(\text{H}_2\text{O})_2](\text{NO}_3)_2$	1059.95	Red	130	49.86 (49.75)	4.18 (4.14)	13.21 (13.30)	5.56 (5.24)	3.40 (3.47)	210
Fe(III)	$[\text{Fe}(\text{C}_{22}\text{H}_{30}\text{N}_4\text{O}_3\text{S})_2(\text{H}_2\text{O})_2](\text{NO}_3)_3$	1118.87	Dark brown	95	47.23 (47.34)	3.96 (3.90)	13.77 (13.61)	4.99 (4.73)	3.22 (3.01)	251
L4	$\text{C}_{12}\text{H}_{11}\text{N}_3\text{O}_2\text{S}$	261.30	Pale yellow	120	55.16 (54.80)	4.24 (4.00)	16.08 (15.80)	–	–	–
Zn(II)	$[\text{Zn}(\text{C}_{12}\text{H}_{11}\text{N}_3\text{O}_2\text{S})_2(\text{H}_2\text{O})_2](\text{NO}_3)_2$	748.04	Pale yellow	130	38.54 (38.41)	3.50 (3.52)	14.98 (15.12)	8.74 (8.43)	4.82 (4.71)	210
Cu(II)	$[\text{Cu}(\text{C}_{12}\text{H}_{11}\text{N}_3\text{O}_2\text{S})_2(\text{H}_2\text{O})_2](\text{NO}_3)_2$	746.19	Greenish yellow	165	38.63 (38.48)	3.51 (3.54)	15.02 (15.21)	8.52 (8.61)	4.83 (4.61)	175
Ni(II)	$[\text{Ni}(\text{C}_{12}\text{H}_{11}\text{N}_3\text{O}_2\text{S})_2(\text{H}_2\text{O})_2](\text{NO}_3)_2$	741.34	Green	160	38.88 (38.74)	3.53 (3.52)	15.12 (15.31)	7.92 (7.81)	4.86 (4.92)	140
Co(II)	$[\text{Co}(\text{C}_{12}\text{H}_{11}\text{N}_3\text{O}_2\text{S})_2(\text{H}_2\text{O})_2](\text{NO}_3)_2$	741.58	Violet	125	38.87 (38.80)	3.53 (3.70)	15.11 (15.37)	7.95 (7.86)	4.86 (4.59)	165
Fe(III)	$[\text{Fe}(\text{C}_{12}\text{H}_{11}\text{N}_3\text{O}_2\text{S})_2(\text{H}_2\text{O})_2](\text{NO}_3)_3$	800.49	Dark brown	150	36.01 (36.32)	3.27 (3.41)	15.75 (15.71)	6.98 (7.03)	4.50 (4.62)	260

TABLE-3
CHARACTERISTIC INFRARED ABSORPTION FREQUENCIES (cm⁻¹) OF
L1 AND L2 LIGANDS AND ITS COMPLEXES

Assignment	L1	L1-Zn	L1-Cu	L1-Ni	L1-Co	L1-Fe
v(NO ₃)	-	1384 vs	1382 vs	1381 vs	1383 vs	1380vs
v(H ₂ O)	-	3000- 3696 br	-	3000- 3713 br	3000- 3696 br	3000- 3687 br
v(OH,NH, NH ₂)	3438 w, 3260 w, 3133 w	3326 sh, 3189 sh, 3062 sh	3424 m	3321 sh, 3321 sh	3259 m, 3134 m	3288 sh, 3166 sh
v(C=N, C=C)	1631 w, 1573 s	1627 w, 1568 s	1622 w, 1572 s	1627 w, 1577 w	1643 m, 1574 s	1626 w, 1571
v(C=S)	1114 s	1111 s	1107 s	1108 s	1114 s	1111 s
v(C-H)	-	2365 w	2362 s	2363 m	2364 w	2363 m
v(M-N)	-	546 w	546 w	505 w	542 w	539 w
v(M-S)	-	496 w	472 w	410 w	469 m	470 w
	L2	L2-Zn	L2-Cu	L2-Ni	L2-Co	L2-Fe
v(NO ₃)	-	1381 w	1381m	1381m	1381m	1387 s
v(H ₂ O)	-	3000- 3656 br	3000- 3655 br	3000- 3652 br	3000- 3668 br	3000- 3652 br
v(OH,NH, NH ₂)	3393 br, 3225 m	3203 m, 3055 w	3181m, 3004 w	3222 m, 3053 w	3229 m, 3052 w	3386w, 3224 w
v(C=O)	1695 sh, 1649 s	1683 sh, 1646 m	1683 m, 1644 s	1669 sh, 1646 sh	1702 sh, 1667 s	1683 sh, 1646 m
v(C=N, C=C)	1603 w, 1556 w, 1513 w	1600 sh, 1559 m, 1507 w	1601 m, 1556 sh	1698 w, 1555 m, 1505 m	1595 w, 1541 m, 1505 s	1601 m, 1552 m, 1507 w
v(M-O)	-	583 m	592 m	578 m	578 m	594 w
v(M-N)	-	499 m	507 w	498 w	496 m	-

Zn(II), Cu(II), Ni(II), Co(II) and Fe(III), which indicate the participation of the carbonyl group in the complexation process²³. Generally the observed shift of this band was small. This may result from two opposing factors:

- Coordination at C=O would cause a shift to lower frequencies and,
- The breaking of inter-and intramolecular hydrogen bonds frequencies would cause a shift to higher frequencies²³.

The stretching or deforming bands of the coordinate bonds are generally found at the low-frequency end of the infrared range, both the heavy metal atom and the nature of the coordinate bond being responsible for these bands. Coordination complexes frequently contain metal-oxygen or metal-nitrogen, or metal-sulphur bonds, but the absorption bands associated with these bonds are normally difficult to assign empirically since their position is not only dependent on the metal but also on the ligand and

TABLE-4
CHARACTERISTIC INFRARED ABSORPTION FREQUENCIES (cm⁻¹) OF
L3 AND L4 LIGANDS AND THEIR COMPLEXES

Assignment	L3	L3-Zn	L3-Cu	L3-Ni	L3-Co	L3-Fe
v(NO ₃)	-	1383	1381	1382	1383	1386
v(H ₂ O)	-	3200- 3672 br	3200- 3668 br	3200- 3708	3200- 3668 br	3000- 3668 br
v(OH, NH, NH ₂)	3394 br	-	-	-	-	-
v(C=O)	1723 s, 1604 m,	1734 s	1733 s	1733 s	1733 s	1721 m
v(C=N, C=C)	1555 m, 1503 s	1625 w, 1593 m, 1508 w	1654 w, 1597 m, 1501 m	1624 w, 1595 m, 1504	1625 m, 1593 m, 1506	1602 s, 1557 m, 1500 s
v(M-O)	-	520 w	518 w	570 w	520 w	542 w
v(M-N)	-	487 w	486 w	493 w	488 w	515 w
	L4	L4-Zn	L4-Cu	L4-Ni	L4-Co	L4-Fe
v(NO ₃)	-	1381 s	1385 s	1385 s	1385 s	1384 s
v(H ₂ O)	-	3000- 3636 br	3000- 3638 br	3000- 3604 br	3000- 3635 br	3000- 3644 br
v(OH,NH, NH ₂)	3391 m, 3282 m, 3146 m	3315 m, 3163 m	3375 m, 3178 m	3341 m, 3185 m	3311 m, 3170 m	3333 m, 3212 w
v(C=O)	1749 vs,	1748 m	1723 w	1655 s	1748 m	1723 w,sh, 1687 w,sh
v(C=N, C=C)	1621 s, 1504 m	1612 s, 1510 m	1610 s, 1495 w	1607 s, 1503 s	1618 s, 1508 m	1604 m, 1508 w
v(C=S)	1119 s	1121 s	1120 m	1121 s	1120 m	1123 m
v(M-O)	-	594 w	573 w	604 m	596 w	623 m
v(M-N)	-	482 m	476 m	484 w	483 m	482 w

in addition, coupling with other vibration modes often occurs²⁴. By comparing the spectrum of the free ligand with that of the complex, metal-ligand vibrations may often be identified. Since some ligand vibrations may become infrared-active on forming the complex, it is not uncommon for no unambiguous assignments to be made by this comparison. The stretching vibration of M-O, M-N and M-S were listed in Tables 3 and 4.

Thermal analysis: The thermal analysis technique of thermogravimetry (TG) is one in which the change in sample mass is recorded as a function of temperature. The water content in the formed complexes was determined using gravimetric analysis²⁵. The decomposition temperature for all complexes indicate that, the H₂O molecules present in the coordination sphere of the complexes. The % of the H₂O which librated at the decomposition temperature was in good agreement with the result obtained by using (C, H, N, M) analysis, Tables 1, 2, 5. The thermogravimetric studies of the complexes gave more insight on their molecular structure. The

TABLE-5
DTA AND TG ANALYSIS OF THE SYNTHESIZED Cu-COMPLEXES

Complex	T (°C)	Wt. loss (%)		ΔE	Assignment
		Calcd.	Found		
L1-Cu	342 (exo)	74.45	74.01	10.08	Ligand decomposition
	458 (exo)	16.89	16.62	22.78	NO ₃ ⁻ liberation
	70 (exo)	-	-	1.75	Phase transition
L2-Cu	134 (exo)	4.16	4.30	10.66	Coordinated H ₂ O liberation
	336 (exo)	74.19	74.01	-	Ligand decompose
	445 (exo)	14.32	14.23	27.76	NO ₃ ⁻ liberation
L3-Cu	148 (exo)	3.38	3.51	5.50	Coordinated H ₂ O liberation
	241 (exo)	79.00	78.93	10.29	Ligand decompose
	492 (exo)	11.65	11.44	20.29	NO ₃ ⁻ liberation
L4-Cu	193 (exo)	4.83	4.61	14.5	Coordinated H ₂ O liberation
	440 (exo)	70.04	70.25	-	Ligand decompose
	495 (exo)	16.62	16.80	10.44	NO ₃ ⁻ liberation

thermogravimetric curves of the Cu(II) complexes showed that, Cu(II)-L2 exhibited a well-defined exothermic peak at 70 °C at DTA thermogram without any weight loss in TG thermogram. This could be probably due to some phase transition in solid state structure. Cu-L2, Cu-L3 and Cu-L4, complexes gave a well-defined exothermic peak at temperature peak 134, 148 and 193 °C, respectively. This could due to the liberation of coordinated water^{26,27}. Such a peak was well observed in the TG curves. The % obtained from the TG thermograms was go well with the data obtained by C, H, N, M analysis. The exothermic peak which appeared at 458, 492, 495, 445 °C for all Cu(II) complexes could be due to the liberation of NO₃⁻ (Table-5). The ligand decomposition peak appeared at 342, 241, 440 and 336 °C as exothermic peak for L1, L3, L4, L2 ligands, respectively. The decomposition product % which obtained from the TG thermogram go well with the calculated % for the postulated structure (**Scheme-II**). The obtained results suggested the following thermal stability order of the different species:

(1) Thermal stability of the coordinated water: Cu(II)-L4 > Cu(II)-L3 > Cu(II)-L2

(2) Thermal stability of the nitrate group: Cu(II)-L4 > Cu(II)-L3 > Cu(II)-L1 > Cu(II)-L2

(3) Thermal stability of the ligand: Cu(II)-L4 > Cu(II)-L1 > Cu(II)-L2 > Cu(II)-L3

The highest stability of all constituents of the Cu(II)-L4 complexes may be due to the perfect structure of this complexes, which obtained from the octahedron structure with six-membered ring chelation through O and N atom, which don't allowed in the other complexes. The activation energies

of the thermal decomposition steps have been calculated from the data obtained from the DTA thermograms using the Piloyan *et al.* method²⁸ (Table-5). It is worth mentioning that E_{act} of the coordinated H_2O and nitrate group has the following order:

(1) E_{act} of the coordinated H_2O : Cu(II)-L4 > Cu(II)-L2 > Cu(II)-L3

(2) E_{act} of the nitrate group: Cu(II)-L1 > Cu(II)-L3 > Cu(II)-L2 > Cu(II)-L4

Mössbauer spectroscopy: A Mössbauer spectrum, in general, reflects the nature and the strength of the hyperfine interaction. The electric monopole interaction affects the position of the resonance lines on the Doppler velocity (energy) scale and gives rise to the so-called isomershift (chemical shifts) δ . The electric quadrupole and magnetic dipole interaction split resonance lines which originate from transitions between degenerate nuclear levels; the electric quadrupole splitting ΔE_Q and the magnetic splitting ΔE_m are the resulting Mössbauer parameters. Most valuable chemical information can be extracted from these three "Mössbauer parameters" δ , ΔE_Q , ΔE_m .

The Mössbauer spectra of Fe(III) complexes (Fig. 1 and Table-6), were obtained at room temperature, which gives velocity range from -5 to +5 mm/s. The spectra of all complexes have two peaks with $\delta = +0.213$, +0.2, +0.2 and +0.26 for L4, L1, L2 and L3, respectively and quadrupole splitting $\Delta E_Q = 0.58$, 0.75, 0.72 and 0.703, respectively. From the value of the isomer shift (δ) indicates that the Fe(III) complexes may be found in one of the two possibilities:

(a) low spin Fe(II) complexes, or

(b) high spin Fe(III) complexes,

meanwhile the values of the magnetic susceptibility (μ_{eff}) (Table-6), confirmed the argument (b), also the values of ΔE_Q indicate that we have distorted octahedral structure²⁹⁻³².

TABLE-6
MÖSSBAUER DATA OF THE SYNTHESIZED Fe-COMPLEXES

Complex	δ	ΔE_Q	μ	Assignification
L1-Fe	0.200	0.750	5.4	High spin Fe(III) complexes
L2-Fe	0.200	0.720	5.1	High spin Fe(III) complexes
L3-Fe	0.260	0.703	5.3	High spin Fe(III) complexes
L4-Fe	0.213	0.580	5.3	High spin Fe(III) complexes

Molecular modeling: The postulated spatial arrangements have been confirmed using the molecular modeling program AlchemyIII. The program has been applied on many different arrangements for each ligand, the most stable one (which gave the minimum molecular energy) being presented in **Scheme-I**.

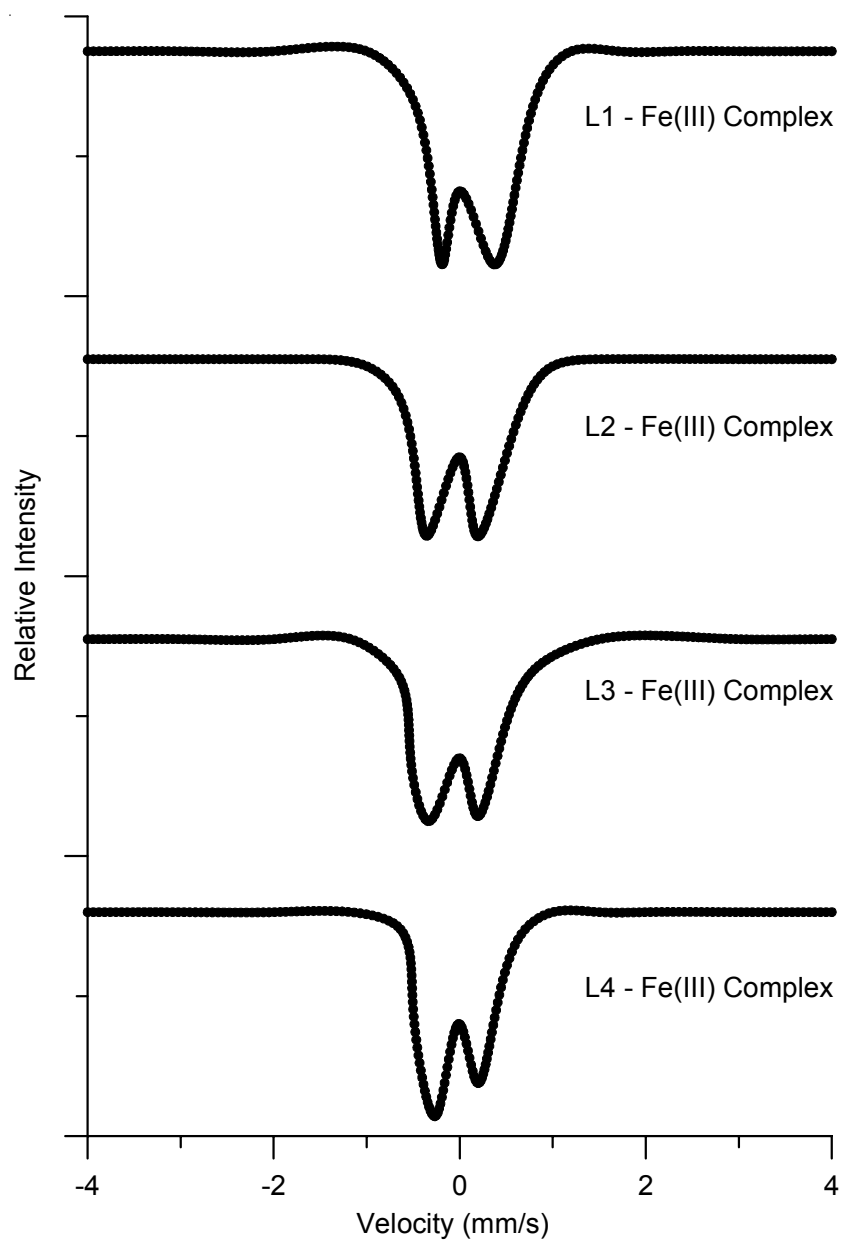
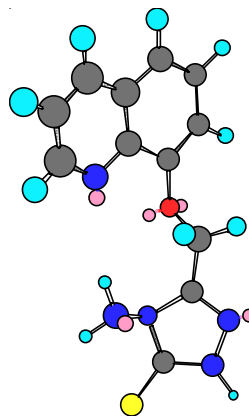
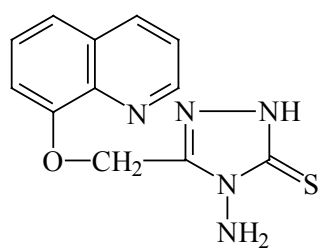
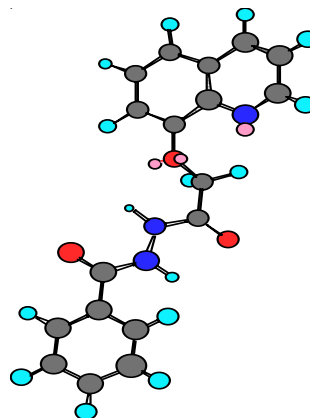
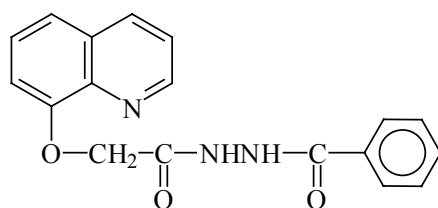


Fig. 1. Mössbauer diagram for Fe(III) complexes

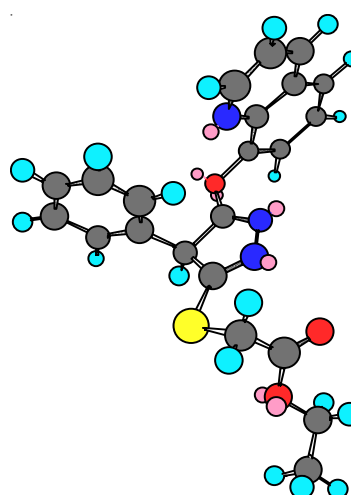
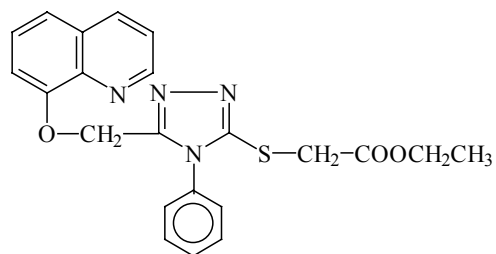
Finally, from the elemental analysis, conductance, IR, thermal analysis, Mössbauer spectra and molecular modeling calculation, could be assignment the structure of the formed complexes from the ligands under investigation as shown in the **Scheme-II** (as an example).



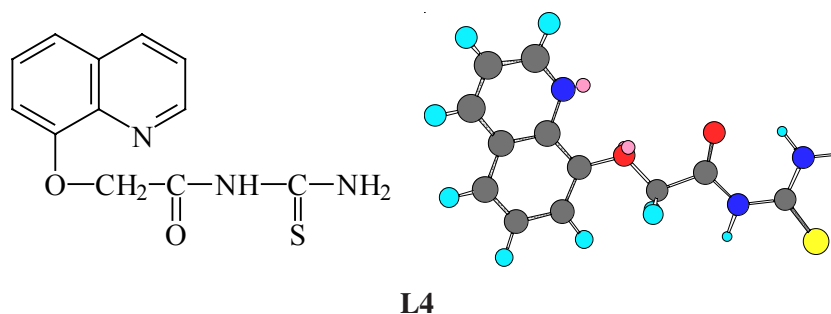
L1



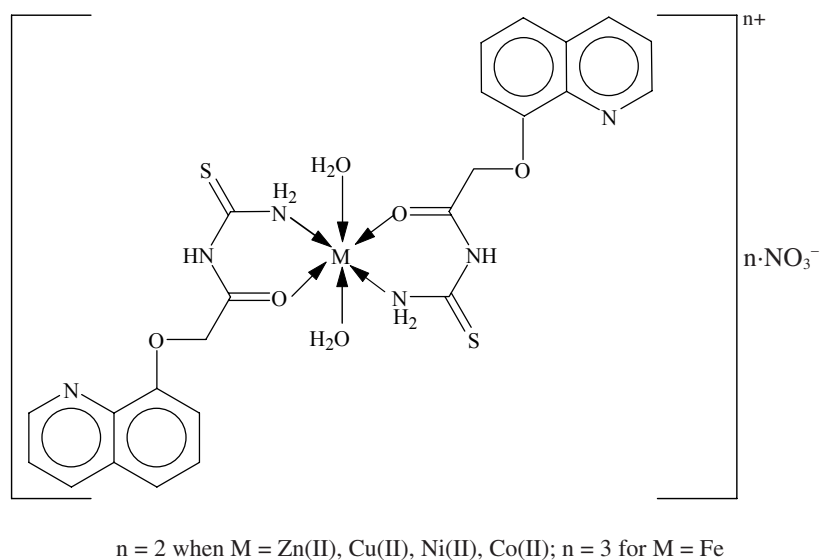
L2



L3



Scheme-I. The ligands configuration and their molecular modeling pictures.



Scheme-II. The postulated structures of the metal complexes of L4 ligand.

Antimicrobial activity: In general, most of the tested synthesized compounds improve significantly the antimicrobial activity against the studied microorganisms, at concentration of 50 and 100 ppm (Table-7).

(1) Metal complexes of the studied ligands (L1, L2, L3 and L4) with the metal ions: Zn^{2+} , Cu^{2+} , Ni^{2+} , Co^{2+} and Fe^{3+} generally enhanced the antimicrobial properties, may be due to the increasing of the ionic character of the complexes rather than the ligands, which facilitate the penetration of the compounds through the bacterial wall.

(2) Zn(II) complexes gave the lowest activity towards the studied microorganisms.

TABLE-7
ANTIMICROBIAL ACTIVITIES OF THE LIGANDS AND
THEIR COMPLEXES

Compd.	Gram-positive bacteria		Gram-negative bacteria	
	<i>Bacillus subtilis</i>		<i>Escherichia coli</i>	
	50 ppm	100 ppm	50 ppm	100 ppm
L1	-	++	+	++
L1- Zn(II)	+	++	+	+
L1- Cu(II)	++	+++	++	+++
L1- Co(II)	+	++	++	++
L1- Ni(II)	+	++	+	++
L1- Fe(III)	++	+++	++	+++
L2	+	++	+	++
L2- Zn(II)	+	+	+	+
L2- Cu(II)	++	+++	+++	+++
L2- Co(II)	+	++	+	++
L2- Ni(II)	+	++	+	++
L2- Fe(III)	+	++	++	+++
L3	-	+	++	++
L3- Zn(II)	-	+	++	++
L3- Cu(II)	+	++	+++	+++
L3- Co(II)	-	+	+	++
L3- Ni(II)	-	+	+	++
L3- Fe(III)	+	++	+++	+++
L4	+	++	++	+++
L4- Zn(II)	++	++	++	++
L4- Cu(II)	+++	++++	+++	++++
L4- Co(II)	++	++	++	+++
L4- Ni(II)	++	++	++	+++
L4- Fe(III)	+++	+++	+++	++++

(-) = inactive, (+) = slightly active, (++) = moderately active, (+++) = active, (++++) = very active

(3) The antimicrobial activity of the synthesized complexes could be summarized as follow:

- for L1 complexes: L1 < Fe(III) > Co(II) = Ni(II) < Cu(II) > Zn(II)
- for L2 complexes: L2 < Fe(III) > Co(II) = Ni(II) < Cu(II) > Zn(II)
- for L3 complexes: L3 < Fe(III) > Co(II) = Ni(II) < Cu(II) > Zn(II)
- for L4 complexes: L3 < Fe(III) > Co(II) = Ni(II) < Cu(II) > Zn(II)

From the previous trends we conclude that:

- Metal complexes have antimicrobial activity higher than their ligands
- Cu(II) and Fe(III) complexes gave the maximum activities
- All complexes are biologically active at 100 ppm concentration meanwhile at 50 ppm, L3, Zn(II)-L3, Ni(II)-L3 and Co(II)-L3 compounds are inactive.

(d) Generally, L4 complexes > L1 complexes > L2 complexes > L3 complexes according to its antimicrobial activities.

(6) The obtained results giving some idea about the importance of the complex formation for getting more potent antimicrobial agents and metal ions play many important roles in biological system¹⁻⁷.

REFERENCES

1. S.N. Sawhney, S. Bhutani and D. Vir, *Indian J. Chem.*, **25B**, 667 (1989).
2. N. Imaki, Y. Takuma and M. Oishi, Eur. Pat., 335046; *Chem. Abstr.*, **112**, 158074t (1990).
3. G. Palazzino, L. Cecchi, F. Melani, V. Colotta, G. Filacchioni, C. Martini and A. Lucacchini, *J. Med. Chem.*, **107**, 45 (1987).
4. N.G. Latour and R.E. Reeves, *Exp. Parasitol.*, **17**, 203 (1965).
5. S. Ahmed, R.C. Gupta, K. Shanker, R. Nath, K.B. Bhargava and K. Kisher, *J. Indian Chem. Soc.*, **56**, 1265 (1979).
6. R.V. Davis, *Chem. Abstr.*, **97**, 23645f (1982).
7. J.M. McCall, *J. Med. Chem.*, **29**, 133 (1986).
8. A.M. Khalil, N.S. Habib, A.M. Farghaly and O.A. El-Sayed, *Arch. Pharm. (Weinheim)*, **324**, 249 (1995).
9. R.J. Lukens and D.C. Torgeson, *Fungicides*, Academic press, New York, Vol. 2, Ch. 9 (1969).
10. K. Takemoto, *J. Macromol. Sci. Rev. Macromol. Chem.*, **5**, 29 (1970).
11. J.R. Parrish and R. Stevenson, *Anal. Chim. Acta*, **70**, 189 (1974).
12. F. Vernon, *Chem. Ind. (London)*, **6**, 634 (1977).
13. F. Hasegawa, K. Fukukawa, H. Toyoda, K. Sato and I. K. Takahashi, *Carcinogenesis*, **10**, 711 (1989).
14. Y. Shen, C.P. Chen and S. Roffler, *Life. Sci.*, **64**, 813 (1999).
15. J-M. Ouyang and Z-M. Zhang, *Thin Solid Films*, **363**, 134 (2000).
16. J-M. Ouyang, W-H. Ling, C. Yang, Y. Li and G. Yu, *Mater. Sci. Eng.*, **B85**, 247 (2001).
17. E. La Voie, S. Dolan, P. Little, C-X. Wang, B.M. Way and Ca. McQueen, *Carcinogenesis*, **12**, 217 (1991).
18. M.I. Williams, G. DuBois, D.R. Boyel, R.J.H. Davies, L. Hamilton, J.I. McCullough and P.J. van Bladeren, *Mutat. Res.*, **278**, 277 (1992).
19. E.S. Ibrahim, S.A. Sallam, A.S. Orabi, B.A. El-Shetary and A. Lentz, *Montashefte Für Chemie*, **129**, 159 (1998).
20. N.F. Curtis and Y.M. Curtis, *Inorg. Chem.*, **4**, 804 (1965).
21. K.A. Jensen and U. Anthoni, *Acta Chem. Scand.*, **24**, 2055 (1970).
22. K. Nakamoto, *Infrared and Raman Spectra of Inorganic and Coordination Compounds*, Wiley Interscience, New York, edn. 3 (1978).
23. A.L. Ram, M.N. Singh and S. Das, *Synth. React. Inorg. Met-Org. Chem.*, **16**, 513 (1986).
24. G. Socrates, *Infrared Characteristic Group Frequencies*, John Wiley, Great Britain (1980).
25. A.I. Vogel, *Textbook of Quantitative Inorganic Analysis*, Longman, London, edn. 4 (1978).
26. A.S. Orabi, *Montashefte Für Chemie*, **129**, 1139 (1998).
27. T.H. Rakha, A.A. El-Asmy, M.M. Mostafa and A. El-Kourshy, *Transition Met. Chem.*, **12**, 125 (1987).
28. G.O. Piloyan, I.D. Ryabchikov and O.S. Novikova, *Nature*, **212**, 1229 (1966).
29. N.N. Greenwood and T.C. Gibb, *Mössbauer Spectroscopy*, Chapman and Hall, London, edn. 1 (1971).
30. P.B. Moon, *Proc. Phys. Soc.*, **63**, 1189 (1950).
31. D.A. Shirley, *Rev. Mod. Phys.*, **36**, 339 (1964).
32. A. J. Freeman and R.E. Waston, *Phys. Rev.*, **131**, 2566 (1963).
33. W.J. Geary, *Coord. Chem. Rev.*, **7**, 81 (1971).